Conf-940388--1

LA-UR-94-972

Title: **THEORETICAL AND EXPERIMENTAL INVESTIGATIONS OF ELASTIC SCATTERING SPECTROSCOPY AS A POTENTIAL DIAGNOSTIC FOR TISSUE PATHOLOGIES**

Author(s): James Boyer, Judith R. Mourant, and Irving J. Bigio

Submitted to: Advances in Optical Imaging and Photon Migration
Orlando, Florida
March 21-23, 1994

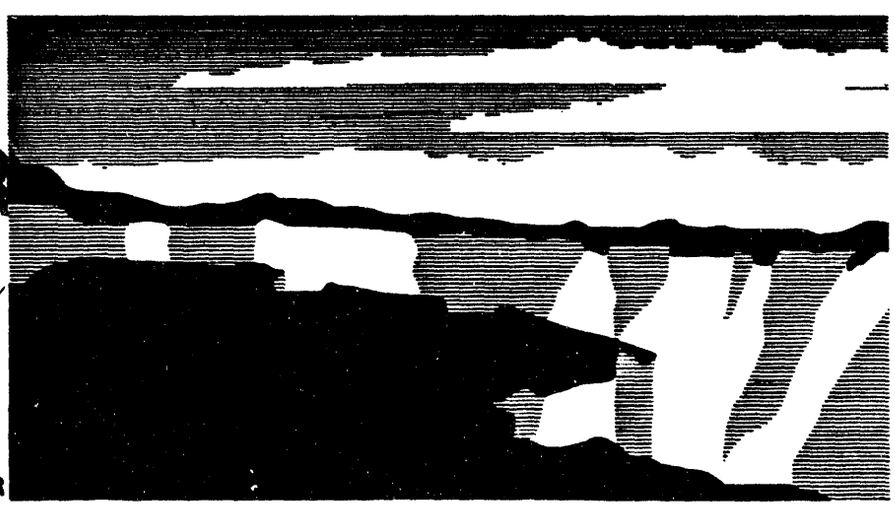

Los Alamos
NATIONAL LABORATORY

Form No. 836 R5
ST 2629 10/91

Theoretical and experimental investigations of elastic scattering spectroscopy as a potential diagnostic for tissue pathologies.

James Boyer, Judith R. Mourant, and Irving J. Bigio
Laser Science and Applications Group, MS E543
Los Alamos National Laboratory
Los Alamos, New Mexico 87545
(505) 667-0041

Abstract

The spectral distribution of the diffuse reflectance of five sizes of polystyrene microspheres has been measured with an elastic scatter spectrometer designed for optical biopsy of living tissue. The microsphere sizes are representative of the suspected scattering centers in living tissue. The experiment data are discussed and interpreted in the framework of Mie scattering theory and Monte-Carlo transport analysis. Present results support the assertion that Mie theory is necessary to describe the spectral features of elastic scatter spectroscopy in tissue.

Introduction

We have built a prototype optical biopsy system (OBS) capable of discriminating among tissue types and conditions. The OBS is based on elastic scatter spectroscopy. Photons entering a tissue may be elastically scattered, inelastically scattered, or absorbed. In general, the scattering-cross-section is about 100 times greater than the absorption-cross-section. It is therefore expected that the amplitude and wavelength distribution of photons emerging from the tissue depend upon the cellular and sub-cellular structure of the tissue as well as the tissue biochemistry. Since changes in cellular architecture are often associated with tissue pathologies, such as malignancy, elastic scatter spectroscopy is a potential diagnostic tool for malignancy and other tissue abnormalities. This system proved successful in an *in vivo* study of patients known to have bladder tissue abnormalities.[1] Figure 1 illustrates the elastic scatter spectra of typical bladder tissues examined in the *in vivo* study. The trace labeled non-tumorous includes both normal and abnormal tissues spectra from one patient. The trace labeled tumorous is the average of the malignant tissue spectra from that patient

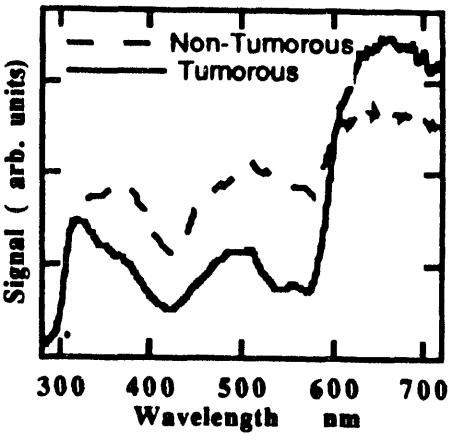

Figure 1. These spectra are averages from one patient.

Most analytical models of the interaction of light with tissue have employed the radiative transport equation or approximations to it such as the P1 approximation (diffusion theory) and the P3 approximation. Alternatively Monte-Carlo simulations have been used. In the P1 and P3 approximations only the first few terms of a spherical harmonic expansion of the light fluence are used. Therefore, these approximations are inaccurate for light distributions which are far from isotropic which is the case for the OBS geometry. The P3 approximation, however, is a significant improvement over the P1 approximation and is in closer agreement with Monte-Carlo simulations.[2] Monte-Carlo simulations are, however, used exclusively in this study.

Cellular components of tissue that are expected to contribute the majority of the elastic scattering events have dimensions comparable with or larger than the wavelengths of the spectral band used to probe the

tissue (300-1000 μ). Therefore, the dominant scattering characteristics are best described by Mie theory or multiple scattering extensions of Mie theory.

Although the particle size to wavelength ratio in tissue is such that Mie theory is applicable, only a few investigators have used Mie theory for the prediction of optical parameters or compared measured values with those predicted by Mie theory. Graaff et al. derived an analytical expression for the reduced scattering cross section $\sigma_S' = \sigma_S(1-g)$ (for a specific range of relative refractive index and size parameter).[3] Measurements of the angular light scattering distribution for a dilute solution of particles agreed with Mie theory predictions for both red blood cells and hollow latex spheres.[4,5] Experimentally measured values of μ_S for a solution of polystyrene spheres were within 20% of the values determined from Mie theory calculations from 300-700 nm.[6]

We are reporting experimental measurements of elastic scatter from suspensions of polystyrene microspheres and initial efforts to model the measured elastic scatter spectra. We used Mie theory to determine the angular and amplitude scattering properties of the spheres and Monte-Carlo computation to describe the resultant photon transport.

Experimental Procedures

We measured the elastic scatter spectra of aqueous suspensions of mono disperse polystyrene spheres of five different radii (0.24, 0.48, 1.02, 1.46, and 1.85 μ) and several concentrations. Concentrations measured ranged from 1 to 0.03% by weight. Corresponding mean particle separation range from 3.8 to 12.2 diameters which is only a few microns for the more concentrated suspensions of the smaller spheres.

The elastic scatter spectrometer is composed of a broad band source (xenon arc lamp) delivered to the specimen by a 500 μ optical fiber and a CCD array spectrometer for analyzing light picked up by a 200 μ fiber in close proximity to the source fiber. Both fibers are placed in contact with or immersed in the specimen as appropriate. Photons entering the specimen interact primarily by multiple scattering off the suspended spheres. Absorption is weak and most photons eventually emerge from the suspension. A small fraction of the photons enter the spectrometer fiber after multiple scattering events and are analyzed in the spectrometer.

The spectral response of the spectrometer, xenon lamp, and fiber are eliminated from the processed spectra by dividing by the signal obtained from a reference diffuse reflector. The procedure is given by the following equation:

$$I(\lambda) = \frac{I_{sig.} - I_{offset\ sig.}}{I_{ref.} - I_{offset\ ref.}}$$

I_{sig} is the spectrometer signal of interest, $I_{offset\ sig.}$ is spectrometer offset when measuring the signal, $I_{offset\ ref.}$ is the offset when measuring the reference, and $I_{ref.}$ is the signal from the diffuse reflector. The offsets arise from the CCD dark current and dc offsets from readout electronics. Figure 2 shows representative spectra.

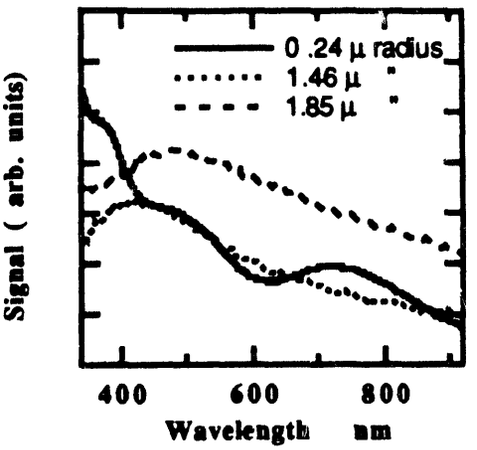

Data Analysis

The sphere suspension were prepared at specific concentration of spheres by weight. In retrospect it would have been better to prepare suspensions of constant particle number density. The Monte-Carlo transport model will assume that $\mu_S = N_S A_S Q_{scat}$ where Q_{scat} is the scattering efficiency of Mie theory, N_S is the sphere number density, and A_S is the sphere cross-sectional-area. The quantity $N_S A_S$ is proportional to R_a^{-1} where R_a is the sphere radius and is a constant for fixed suspension concentration and sphere mass density. It is therefore useful (assuming that detected scatter amplitude is proportional to μ_S) to display the scatter spectra multiplied by the sphere radius as in Figure 3 below.

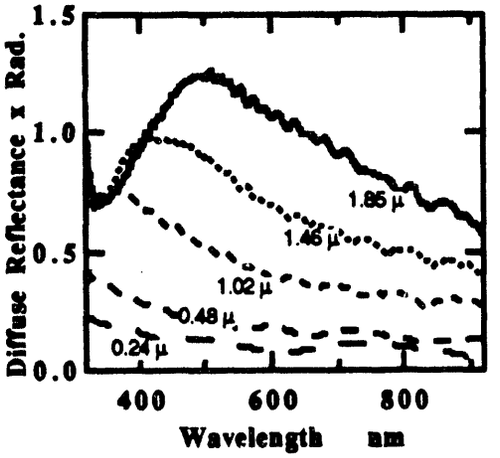

Figure 3. These spectra are for the 1% suspensions of the polystyrene spheres.

Figure 3 shows the character of the scatter spectra for all sizes in 1% suspensions. The spectra of other concentrations are similar. For each concentration, there is a maximum in the scatter spectrum at a wavelength which increases with sphere radius. If the observed scatter signal were strictly proportional to μ_S, the scatter signal would be identical as a function of size parameter ($X = 2\pi n_S R_S/\lambda$). Examination of the observed scatter spectra reveals that the maxims are not the same amplitude and do not occur at the same X. The concentration dependence for the amplitude of the scatter spectra is also weaker than that of μ_S. Figure 4 below, shows the relationship between Q_{ext} and measured elastic scatter spectra for spheres with R_S of 1.85 and 1.46 μ.

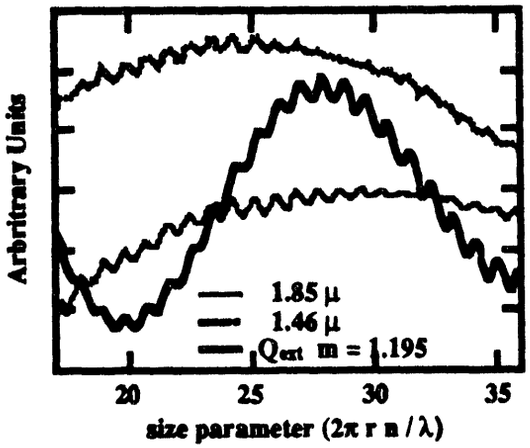

Figure 4. The scatter signals for the 1.46 and 1.85 μ radius spheres have the ripple structure present in Q_{ext}.

The ripple is periodic in X with period dependent on relative refractive index (m), but independent of the sphere radius. This ripple is also present for the smaller spheres and is insensitive to sphere concentration. Mixing suspensions of different size spheres suppresses the ripple. Figure 4 also clearly makes the point that the scatter amplitude does not scale directly with μ_S.

Modeling

The sphere radii are such that Mie theory is necessary to describe the scattering amplitudes and angular distributions. Boren and Huffman give a useful computational algorithm for Q_{ext}, Q_{scat} and the angular distribution of the scatter amplitude.[7] We modified their code to generate cumulative probability distributions for the angular scatter which are used in Monte-Carlo photon propagation computations. The modified code gives the same scatter coefficients as the original for the sample calculation of the authors. The Monte-Carlo propagation code also uses $\mu_S = N_S A_S Q_{scat}$ and $\mu_a = N_S A_S (Q_{ext} - Q_{scat}) + \mu_{am}$ derived from Q_{ext}, Q_{scat}, and the medium absorption (μ_{am}).

The OBS geometry is such that diffusion theory is not applicable. Figure 5 compares a single wavelength photon absorption profile generated by a Monte-Carlo computation with the geometry of the OBS source and detector fibers. It is readily seen that the radiation pattern is far from isotropic at the probe position.

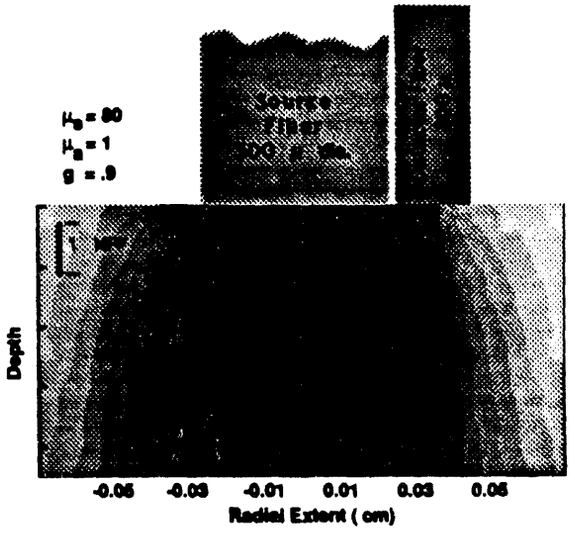

Figure 5. Absorption profile from Monte-Carlo computation using a Henyey-Greenstein phase function.

The Monte-Carlo code is a simplified version of the code distributed by Wang and Jacques.[8] The present code interpolates a table of cumulative probability distribution for the angular scatter from Mie computations. For the OBS simulation, only those photons leaving the medium directly under the spectrometer probe (in practice we count those exiting at the annulus defined by the probe) are counted. The computation is of course repeated for each wavelength.

Several complications in these simulations result from the very low values of absorption coefficients of all constituents of the suspensions relative to μ_S. Since scattering is dominant, the photon experiences many interactions before being absorbed. In initial simulation efforts reported here, the photon was tracked until it was absorbed or escaped from the medium. The consequence was excessive computational time. By keeping track of the number of interactions experienced by the photons entering the detector fiber, it is observed that the mean number of interactions of the detected photons is much smaller than that for a typical photon. Examination of the distribution of the number of interactions may suggest a more efficient termination criterion. The second complication of small μ_a is seen in if a large μ_a is forced. In that case the scatter spectrum tends to follow μ_S closely. The implication is that μ_a needs to be well known which is not the case for the suspensions studied here. This might best be accomplished by introducing a well known absorber

into the suspension. Figure 6 shows two initial efforts at simulation.

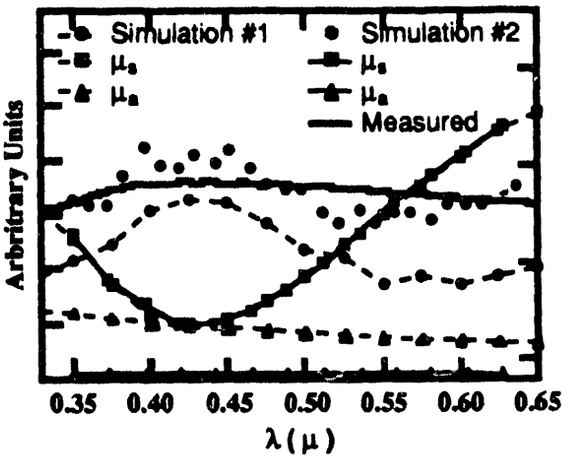

Figure 6. Two simulations of scatter spectra for a suspension of 1.02 μ radius spheres and a measured scatter spectrum.

The simulations in fig. 6 are following μ_s more closely than is the measured spectra although it is to be noted that simulation #2 for which μ_a is much smaller is not so structured. Future simulations will use more realistic values for μ_a and/or be compared to suspensions containing a well characterized absorber. High resolution simulations however, have produced more interesting results. Figure 7 below demonstrates that the ripple structure of Q_{ext} is seen in both the measured spectra and Monte-Carlo simulation. In addition, the period of the ripple structure is correctly predicted.

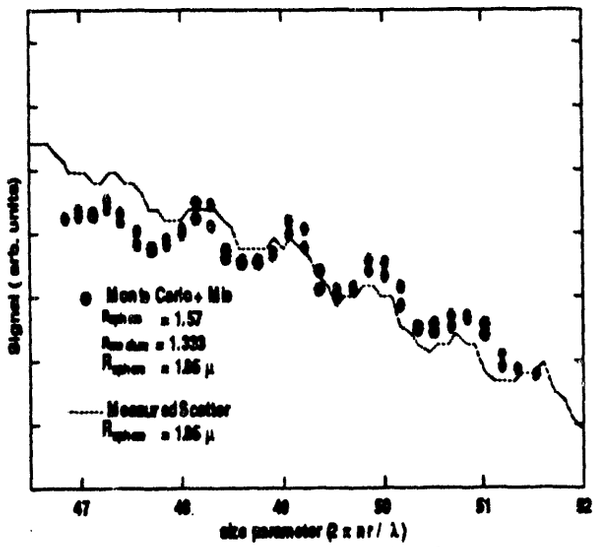

Figure 7. The measured and simulated scatter spectra have the same ripple structure.

The OBS scatter spectra of the sphere solutions all exhibit the ripple structure predicted by Mie scattering theory. The larger amplitude and broader wavelength structure commonly referred to as the interference structure is not obvious in the OBS scatter spectra. The simulations shown here use arbitrary values for μa for reasons already discussed. This may be responsible for the failure to predict the observed scatter spectra. It is also possible that multiple scattering effects play a role, but the sphere concentration dependence in the spectra was too weak to support this explanation. The presence of the ripple structure support the need for incorporating Mie theory into models of photon transport in tissue.

References

[1] "Optical diagnostics based on elastic scattering:recent clinical demonstrations with the Los Alamos Optical Biopsy System", Irving J. Bigio et al., Proceedings of Biomedical Optics Europe 93, Budapest, September, 1993.

[2] W.M. Star,"Comparing the P3-Approximation with Diffusion Theory and with Monte Carlo Calculations of Light Propagation in a Slab Geometry" in Dosimetry of Laser Radiation in Medicine and Biology eds. Muller JG and Sliney DH (1989) 146-154.

[3] R. Graaf, et al. "Reduced light-scattering properties for mixtures of spherical particles: a simple approximation derived from Mie calculations" Applied Opt. 1992 vol. 31 pg. 1370.

[4] J.M. Steinke, and Shephard,"Comparison of Mie theory and the light scattering of red blood cells" Applied Optics 27:4027.

[5] K.B. Strawbridge, and F.R. Hallett,"Polydisperse Mie theory applied to hollow latex spheres: An integrated light-scattering study" Can J Phys 1992 70:401.

[6] A.J. Durkin, S. Jaikumar, R. Richards-Kortum, "Optically dilute absorbing and turbid phantoms for fluorescence spectroscopy of homogeneous and inhomogeneous samples" Applied Spectroscopy 1992 47:2114.

[7] Craig F. Bohren and Donald R. Huffman, Absorption and Scattering of Light by Small Particles (John Wiley & Sons, 1983), Appendix A.

[8] Lihong Wang and Steven L. Jacques, Laser Biology Research Laboratory - 17, University of Texas M.D. Anderson Cancer Center, 1515 Holcombe Blvd., Houston, TX 77030.

DATE
FILMED
5/9/94
END